

ARTICLE

Nondoped-type White Organic Light-Emitting Diode Using Star-Shaped Hexafluorenylbenzene as an Energy Transfer Layer

Jun-sheng Yu^{a*}, Tao Ma^a, Shuang-ling Lou^a, Ya-dong Jiang^a, Qing Zhang^{b*}

a. State Key Laboratory of Electronic Thin Films and Integrated Devices, School of Optoelectronic Information, University of Electronic Science and Technology of China, Chengdu 610054, China

b. Department of Polymer Science, School of Chemistry and Chemical Technology, Shanghai Jiao Tong University, Shanghai 200240, China

(Dated: Received on January 7, 2008; Accepted on June 3, 2008)

White organic light-emitting diodes (WOLEDs) with a structure of indium-tin-oxide (ITO)/N,N'-bis-(1-naphthyl)-N,N'-diphenyl-(1,1'-biphenyl)-4,4'-diamine (NPB)/1,2,3,4,5,6-hexakis(9,9-diethyl-9H-fluorene-2-yl)benzene (HKEthFLYPh)/5,6,11,12-tetraphenylnaphthalene (rubrene)/tris(8-hydroxyquinoline) aluminum (Alq₃)/Mg:Ag were fabricated by vacuum deposition method, in which a novel star-shaped hexafluorenylbenzene HKEthFLYPh was used as an energy transfer layer, and an ultrathin layer of rubrene was inserted between HKEthFLYPh and Alq₃ layers as a yellow light-emitting layer instead of using a time-consuming doping process. A fairly pure WOLED with Commissions Internationale De L'Eclairage (CIE) coordinates of (0.32, 0.33) was obtained when the thickness of rubrene was 0.3 nm, and the spectrum was insensitive to the applied voltage. The device yielded a maximum luminance of 4816 cd/m² at 18 V.

Key words: White organic light-emitting diode, Star-shaped hexafluorenylbenzene, 1,2,3,4,5,6-hexakis(9,9-diethyl-9H-fluorene-2-yl)benzene, Energy transfer, Ultrathin layer

I. INTRODUCTION

Since Tang and Vanslyke succeeded in fabricating a high efficient green-light emissive organic light-emitting diodes (OLEDs) driven by low direct bias voltage in 1987 [1], OLEDs have been extensively investigated and significantly improved over the past two decades. Due to the superior achieved performance, OLEDs are potential candidates not only for next generation displays, but also for solid state lighting applications which require high efficiency and low operating voltage. Through proper material design/choice and device fabrication, various colors of bright luminance have been developed for use in single- or full-color application. Among various colors, white organic light-emitting diodes (WOLEDs) draw particular attention because of their high potential for application in blacking and full color application, as well as in lighting purposes.

So far, a variety of methods have been proposed to achieve the WOLED. These include the mixing of three primary colors from respective layers in a multilayer structure [2-5], the doping of appropriate amount of red, green, and blue dopants in the same host [6], and the microcavity effect of one emission layer [7], use of exciplex formation [8]. Based on these techniques, the authors also have done some work on WOLED [9,10]. Recently, Forrest *et al.* reported white emission from a blue fluo-

rophore with a green and a red phosphorescent dopant, which had a maximum power efficiency of 37.6 lm/W [11]. Although many reports have already been published about white light and full color display, there is still potential to develop novel light-emitting materials and techniques for white and full color devices.

Fluorene-based compounds and polymers with high photoluminescent quantum yield and good charge transport properties have become an important class of materials for OLED applications [12,13]. However, rigid-rod polyfluorenes have a tendency toward a nematic type of packing arrangement and are inherently prone to chain aggregation in the condensed state. Chain aggregation tends to degrade the device performance as crystalline formation destroys film homogeneity and crystal boundaries increase the resistance of the device, eventually leading to an electrical short. The morphological instability of organic electroluminescent (EL) materials is one of the major problems for device application. Star-shaped molecules have been proven to overcome this problem [14-16]. The device performance incorporating star-shaped materials is significantly high, either as charge-transport material or as emitter due to their tendency to form stable amorphous film with a relatively high glass transition temperature (T_g) and improved thermal stability [17,18]. In this work, WOLEDs were fabricated using a novel star-shaped hexafluorenylbenzene as an emissive assistance layer, and the EL properties of the device were investigated.

* Authors to whom correspondence should be addressed. E-mail: jsyu@uestc.edu.cn, qz14@sjtu.edu.cn, Tel.: +86-28-83207157

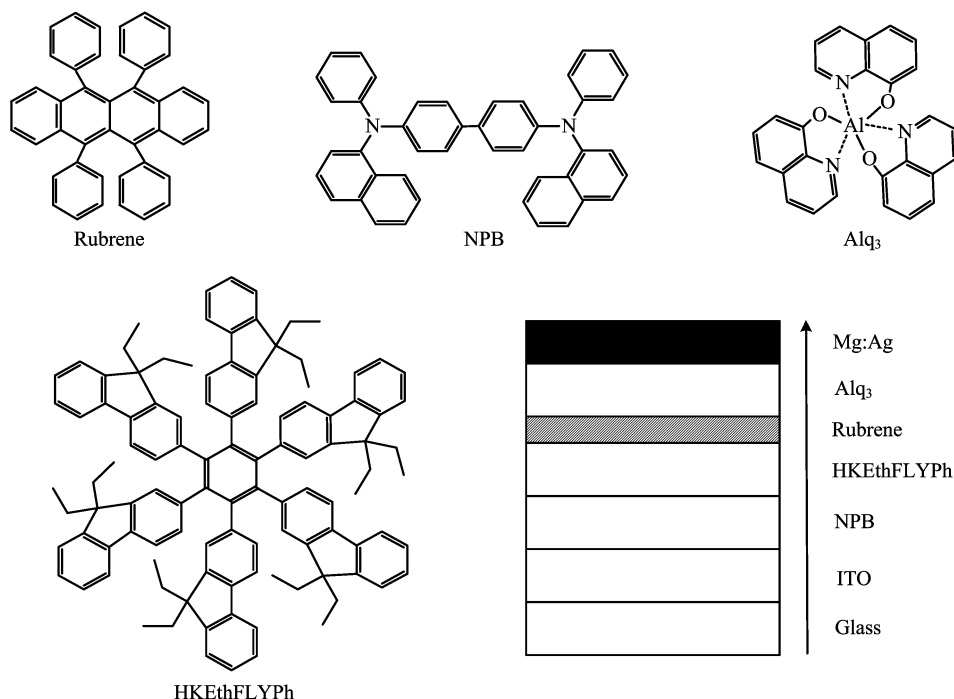


FIG. 1 Molecular structure of the used materials and device architecture.

II. EXPERIMENTS

A novel star-shaped hexafluorenylbenzene 1,2,3,4,5,6-hexakis(9,9-diethyl-9H-fluorene-2-yl)benzene (HKEthFLYPh) which has a six-arm star shaped fluorene structure was synthesized by our group [19-21] and used as an energy transfer layer. The organic materials of N,N'-bis-(1-naphthyl)-N,N'-diphenyl-(1,1'-biphenyl)-4,4'-diamine (NPB), tris(8-hydroxyquinoline)aluminum (Alq₃) and 5,6,11,12-tetraphenylnaphacene (rubrene) were all purchased from Sigma-Aldrich Co. NPB was used as the blue emitting layer (EML) and the hole transporting layer (HTL). Alq₃ and rubrene acted as electron transporting layer (ETL) and yellow EML, respectively.

The fabricated OLEDs had two different configurations, which were ITO/NPB/HKEthFLYPh/Alq₃/Mg:Ag and ITO/NPB/HKEthFLYPh/rubrene/Alq₃/Mg:Ag, respectively. An ITO-coated glass substrate with a sheet resistance of 12 Ω/□ was employed as anode. ITO glasses were ultrasonically cleaned with detergent water, acetone, ethanol, and deionized water for 10 min at each step, and then dried by nitrogen gas blow. Afterwards, the glasses underwent an oxygen plasma treatment for approximately 5 min to enhance the work function of ITO and thus improve its hole injecting capacity [22,23]. All the organic materials were deposited by conventional thermal evaporation in vacuum background at 4 μPa using the OLED-V organic multi-functional vacuum vapor deposition apparatus. Organic material was evaporated at a rate of

about 0.1-0.2 nm/s. Organic film thickness was controlled by an oscillating quartz crystal thickness monitor. After the organic materials deposited, the samples were transferred to another evaporation chamber, and an alloy of Mg and Ag with a ratio of 10:1 was deposited as cathode using a shadow mask. The resulting film thickness was 200 nm.

The absorption spectrum was investigated by a SHIMADZU UV-1700 spectrophotometer. Commissions Internationale De L'Eclairage (CIE) coordination, photoluminescence (PL) and electroluminescent (EL) spectra of these devices were measured with an OPT-2000 spectrophotometer. All the measurements were carried out at room temperature under ambient atmosphere.

Figure 1 shows the molecular structures of used materials and device architecture.

III. RESULTS AND DISCUSSION

Figure 2 shows the UV-Vis absorption and PL spectra of NPB and HKEthFLYPh films. There is a large overlap between HKEthFLYPh (375 nm) emission spectrum and NPB absorption (355 nm) spectrum. As is well known, Förster energy transfer requires sufficient overlap of donor material emission spectrum with acceptor material absorption emission. In PL spectrum of the blend film of HKEthFLYPh:NPB (1:1, wt%), except for the emission of NPB, there was no other emission, therefore we could infer that sufficient energy transfer from HKEthFLYPh to NPB can be obtained.

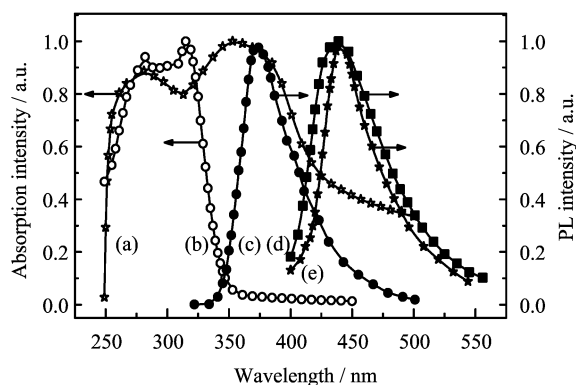


FIG. 2 Absorption and PL spectra of HKEthFLYPh and NPB films. (a) NPB absorption, (b) HKEthFLYPh absorption, (c) HKEthFLYPh emission, (d) HKEthFLYPh:NPB emission, (e) NPB emission.

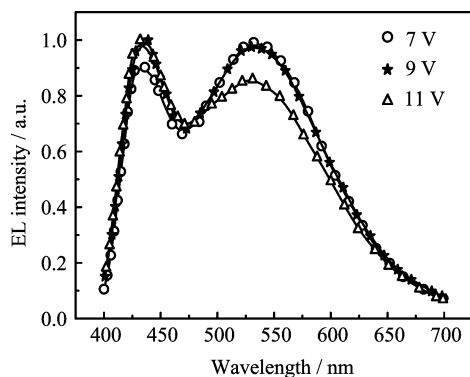


FIG. 3 EL spectra of device A at different driving voltages.

The EL spectrum of triple-layer device A with a structure of ITO/NPB(40 nm)/HKEthFLYPh(10 nm)/Alq₃(50 nm)/Mg:Ag(200 nm) at different driving voltages is shown in Fig.3. There is a significantly broader EL spectrum ranging from 400 nm to 700 nm, which completely covers the whole visible light wavelength region, the EL spectrum contains two primary peaks at 435 and 530 nm. Compared to the PL spectra in Fig.2, it could be concluded that the peak at 435 nm in EL spectrum originates from the emission of NPB layer [24], and there is no emission from HKEthFLYPh. Accordingly, from HKEthFLYPh to NPB, complete energy transfer takes place and HKEthFLYPh emission is thoroughly suppressed. The other EL spectral peak which is located at 530 nm is attributed to the light emission of Alq₃ [25]. The CIE chromaticity coordinates are (0.28, 0.35) at 9 V, which obviously belongs to white light emission. It is worth pointing out that this WOLED showed a slight change in EL spectra with the enhanced driving voltage. e.g., the CIE coordinates change from (0.29, 0.36) at 7 V to (0.28, 0.33) at 11 V, and the peak intensity from the NPB layer increases slightly compared to that of Alq₃ with in-

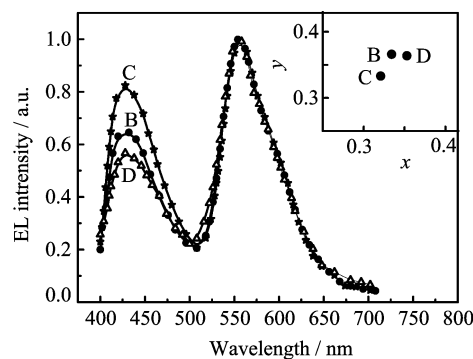


FIG. 4 EL spectra of devices with different rubrene thicknesses. Inset: Chromaticity coordinates of these devices at 7 V. B, C, and D stand for the spectra of devices with 0.1, 0.3, and 0.6 nm thick rubrene, respectively.

creasing bias. Such variation is usually attributed to the shift of recombination zone with different applied voltages. Different voltages corresponding to different electric fields result in different mobility of hole and electron carriers [26]. With the increasing voltage, the ability of organic layers transporting electrons is higher than that of holes, leading to the enhancement of minor charge carriers (electrons) injected into NPB layer to recombine with major charge carriers (holes) and an increase of NPB emission. Moreover, as driving voltage increases, free charge carriers to be injected into the HKEthFLYPh layer are enhanced, which is responsible for increased energy transfer from HKEthFLYPh to NPB. As a result, the relative intensity of blue light emission at 435 nm from NPB is higher.

Although the CIE coordinates of device A are in the white light region, it is slightly shifted from pure white light. In order to obtain more pure white light and improve the stability of the WOLED, an ultrathin layer of rubrene, used as a yellow emissive layer, was inserted between HKEthFLYPh and Alq₃ layers to fabricate ITO/NPB(40 nm)/HKEthFLYPh(10 nm)/rubrene (x nm)/Alq₃(50 nm)/Mg:Ag(200 nm) devices. Figure 4 shows the normalized EL spectra of the devices with different rubrene film thickness. The normalized EL spectra exhibit two primary peaks at 435 and 560 nm, which originate from NPB and rubrene, respectively. The chromaticity of the white emission can be tuned by adjusting the film thickness of rubrene layer, resulting from the direct capture of formed excitons on rubrene molecules and fluorescent emission of radiative decay [27]. Meanwhile, the formed excitons on HKEthFLYPh sequentially transfer their energy via Förster mechanism to NPB [28].

As shown in Fig.4, the emission intensity from rubrene decreases initially and increases relative to that of NPB with the increased thickness of rubrene film. Considering the average diameter of rubrene molecule as ~ 1 nm, less than a homogeneous layer, the ultrathin rubrene "layer" actually should be island-like on

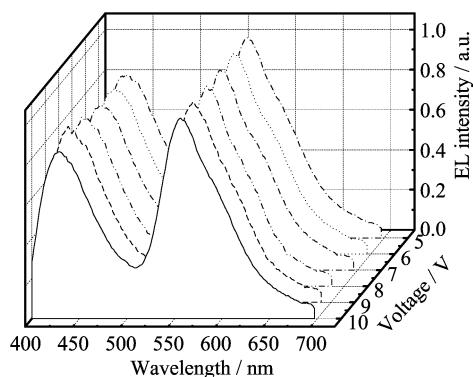


FIG. 5 EL spectra of device C biased at different applied voltages.

HKEthFLYPH film, just like a conventional dope-type device. As Matsumura *et al.* reported [29], the decreasing of light emission from rubrene results from the so-called concentration quenching of fluorescence. In contrast, the increased ratio of rubrene to NPB with the increased thickness of rubrene due to more probability that an electron combined with hole to form a bound exciton and recombined in a light-emitting layer, when the rubrene “layer” became thicker [30]. This conquered the effect of concentration quenching on EL intensity in the case of ultrathin layer thickness over 0.3 nm. Hence, the color of EL emission was changed from yellowish white to white and returned to yellowish white when rubrene layer became thicker as shown in the inset of Fig.4. It can be seen that the CIE coordinates are very close to pure white (0.33, 0.33) at the rubrene thickness of 0.3 nm (device C). A turn-on voltage of 3.5 V and a maximum luminance of 4816 cd/m² at 18 V were obtained.

The EL spectra of device C at different driving voltages are presented in Fig.5, which shows that the peaks of typical EL spectra are located at 435 and 560 nm, corresponding to the CIE coordinates quite close to pure white light (0.33, 0.33). The EL intensity of the WOLED increased with bias voltage, and the ratio of blue to yellow intensity remained almost constant as the bias voltage was enhanced. The high color stability of WOLED was ascribed to the optimized thickness of organic layers and improved charge carrier balance in the recombination zone when rubrene was inserted between HKEthFLYPH and Alq₃ layers. The same phenomenon has been observed in a previous study [31].

Table I presents the CIE coordinates of WOLEDs A and C at different bias voltage. The CIE coordinates of device A at 9 V and device C at 7 V are approximately the purest white light. Blue and yellow lights are completely complementary color, which is ascribed to the CIE coordinates of device C nearer to (0.33, 0.33). Moreover, the CIE coordinates of device C shift slightly, and they are independent of bias voltages.

TABLE I CIE coordinates of WOLED of device A and device C for different bias voltages.

Bias voltage/V	Device A		Device C	
	<i>x</i>	<i>y</i>	<i>x</i>	<i>y</i>
6	0.29	0.35	0.33	0.34
7	0.29	0.36	0.32	0.33
8	0.28	0.35	0.32	0.33
9	0.28	0.35	0.32	0.34
10	0.27	0.33	0.33	0.34

IV. CONCLUSION

A color stable and non-doped WOLED was fabricated using a novel star-shaped hexafluorenylbenzene of HKEthFLYPH as an energy transfer layer. A fairly pure white OLED with CIE coordinates of (0.32, 0.33) was obtained when the thickness of rubrene is 0.3 nm, which was not sensitive to bias voltage. The simple structure of the device also paves the way for the fabrication of WOLED inserted an ultrathin layer of rubrene between HKEthFLYPH and Alq₃ layers, which was used as a yellow light-emitting layer instead of utilizing a doping process.

V. ACKNOWLEDGMENTS

This work was supported by the National Natural Science Foundation of China (No.60425101 and No.20674049), the Program for New Century Excellent Talents in University (No.NCET-06-0812), and the Young Talent Project at University of Electronic Science and Technology of China (No.060206).

- [1] C. W. Tang and S. A. Vanslyke, *Appl. Phys. Lett.* **51**, 913 (1987).
- [2] J. Kido, M. Kimura, and K. Nagai, *Science* **267**, 1332 (1995).
- [3] J. Yu, Z. Chen, M. Sone, S. Miyata, M. Li, and T. Watanabe, *Jpn. J. Appl. Phys.* **40**, 3201 (2001).
- [4] M. Strukelj, R. H. Jordan, and A. Dodabalapur, *J. Am. Chem. Soc.* **118**, 1213 (1996).
- [5] B. W. D'Andrade, M. E. Thompson, and S. R. Forrest, *Adv. Mater.* **14**, 147 (2002).
- [6] J. Kido, H. Shionoya, and K. Nagai, *Appl. Phys. Lett.* **67**, 2281 (1995).
- [7] A. Dodabalapur, L. H. Rotherg, and T. M. Miller, *Appl. Phys. Lett.* **65**, 2308 (1994).
- [8] J. Thompson, R. I. R. Blyth, M. Mazzeo, M. Anni, G. Gigli, and R. Cingolani, *Appl. Phys. Lett.* **79**, 560 (2001).
- [9] J. Wang, Y. D. Jiang, J. S. Yu, S. L. Lou, and H. Lin, *Appl. Phys. Lett.* **91**, 131105 (2007).
- [10] Y. D. Jiang, J. Wang, J. S. Yu, S. L. Lou, and H. Lin, *Jpn. J. Appl. Phys.* **46**, 523 (2007).

- [11] Y. R. Sun, N. C. Giebink, H. Kanno, B. W. Ma, M. E. Thompson, and S. R. Forrest, *Nature* **440**, 908 (2006).
- [12] D. Y. Kim, H. N. Cho, and C. Y. Kim, *Prog. Polym. Sci.* **25**, 1089 (2000).
- [13] U. Sherf and E. J. W. List, *Adv. Mater.* **14**, 477 (2002).
- [14] S. Roquet, P. Leriche, O. Aleveque, P. Frere, and J. Roncali, *J. Am. Chem. Soc.* **128**, 3459 (2006).
- [15] S. A. Ponomarenko, S. Kirchmeyer, A. Elschner, B. Huisman, A. Karbach, and D. Drechsler, *Adv. Funct. Mater.* **13**, 591 (2003).
- [16] K. Okumoto and Y. Shirota, *Chem. Mater.* **15**, 699 (2003).
- [17] A. L. Kanibolotsky, R. Berridge, P. J. Skabara, I. F. Perepichka, D. D. C. Bradley, and M. Koeberg, *J. Am. Chem. Soc.* **126**, 13695 (2004).
- [18] X. H. Zhou, J. C. Yan, and J. Pei, *Org. Lett.* **5**, 3543 (2003).
- [19] G. Saroja, P. Zhang, N. P. Ernsting, and J. Liebscher, *J. Org. Chem.* **69**, 987 (2004).
- [20] M. J. Mio, L. C. Kopel, J. B. Braun, T. L. Gadzikwa, K. L. Hull, R. G. Brisbois, C. J. Markworth, and P. A. Grieco, *Org. Lett.* **4**, 3199 (2002).
- [21] J. Wu, M. D. Watson, L. Zhang, Z. Wang, and K. Mullen, *J. Am. Chem. Soc.* **126**, 177 (2004).
- [22] T. P. Nguyen, P. L. Rendu, N. N. Dinh, M. Fourmigue, and C. Meziere, *Synth. Met.* **138**, 229 (2003).
- [23] Y. T. Tao, E. Balasubramaniam, A. Danel, B. Jarosz, and P. Tomasik, *Appl. Phys. Lett.* **77**, 1575 (2000).
- [24] V. V. N. Ravi Kishore, A. Aziz, K. L. Narasimhan, Narasimhan, N. Periasamy, P. S. Meenakshi, and S. Wategaonkar, *Synth. Met.* **126**, 199 (2002).
- [25] W. C. Shen, Y. K. Su, and L. W. Ji, *Mater. Sci. Eng. A* **445**, 509 (2007).
- [26] W. C. Shen, Y. K. Su, and L. W. Ji, *J. Cryst. Growth.* **293**, 48 (2006).
- [27] G. Cheng, Y. Zhao, Y. F. Zhang, and S. Y. Liu, *Appl. Phys. Lett.* **84**, 4457 (2004).
- [28] R. S. Deshpande, V. Bulovic, and S. R. Forrest, *Appl. Phys. Lett.* **75**, 888 (1999).
- [29] M. Matsumura and K. Furukawa, *Jpn. J. Appl. Phys.* **40**, 3211 (2001).
- [30] B. W. D'Andrade and S. R. Forrest, *J. Appl. Phys.* **94**, 3101 (2003).
- [31] T. Tsuji, S. Naka, H. Okada, and H. Onnagawa, *Appl. Phys. Lett.* **81**, 3329 (2002).